The EMBO Journal Vol.17 No.18 pp.5273–5285, 1998

Crystal structure of the amphiphysin-2 SH3 domain and its role in the prevention of dynamin ring formation

D.J.Owen, P.Wigge, Y.Vallis, J.D.A.Moore, P.R.Evans and H.T.McMahon[1]

MRC Laboratory of Molecular Biology, Hills Road, Cambridge CB2 2QH, UK

[1]Corresponding author

D.J.Owen and P.Wigge contributed equally to this work

The amphiphysins are brain-enriched proteins, implicated in clathrin-mediated endocytosis, that interact with dynamin through their SH3 domains. To elucidate the nature of this interaction, we have solved the crystal structure of the amphiphysin-2 (Amph2) SH3 domain to 2.2 Å. The structure possesses several notable features, including an extensive patch of negative electrostatic potential covering a large portion of its dynamin binding site. This patch accounts for the specific requirement of amphiphysin for two arginines in the proline-rich binding motif to which it binds on dynamin. We demonstrate that the interaction of dynamin with amphiphysin SH3 domains, unlike that with SH3 domains of Grb2 or spectrin, prevents dynamin self-assembly into rings. Deletion of a unique insert in the n-Src loop of Amph2 SH3, a loop adjacent to the dynamin binding site, significantly reduces this effect. Conversely, replacing the n-Src loop of the N-terminal SH3 domain of Grb2 with that of Amph2 causes it to favour dynamin ring disassembly. Transferrin uptake assays show that shortening the n-Src loop of Amph2 SH3 reduces the ability of this domain to inhibit endocytosis *in vivo*. Our data suggest that amphiphysin SH3 domains are important regulators of the multimerization cycle of dynamin in endocytosis.

Keywords: clathrin/endocytosis/synaptic vesicle/synaptojanin/transferrin

Introduction

A major pathway for endocytosis occurs through a clathrin-mediated process involving the GTPase dynamin (for reviews see DeCamilli *et al*., 1995; McClure and Robinson, 1996). It is essential for the internalization of receptor–ligand complexes and the maintenance of membrane identity in all cells, as well as being an important pathway of synaptic vesicle recycling in neurons (Maycox *et al*., 1992; Morris and Schmid, 1995). Molecules destined to be internalized are concentrated in clathrin-coated pits which are then 'pinched off' to form vesicles. Steps leading to this include the formation of a curved clathrin lattice, providing the mechanical scaffold for the forming vesicle, and the recruitment of the GTPase dynamin to the neck of the forming vesicle (Pearse and Robinson, 1990; DeCamilli *et al*., 1995). The importance of dynamin is illustrated by the paralytic phenotype of the *shibire* mutant in *Drosophila*, in which a late stage of endocytosis is blocked (Poodry and Edgar, 1979; Kosaka and Ikeda, 1983). The morphology of invaginated pits in this mutant strain, visualized by electron microscopy, strikingly resembles that of nerve terminals treated with the non-hydrolysable analogue of GTP, GTPγS (Takei *et al*., 1995). The necks of these endocytosing vesicles are decorated with rings of dynamin, suggesting that dynamin serves a molecular 'garrotting' role in the pinching-off stage, possibly controlled by a conformational change upon GTP hydrolysis (Takei *et al*., 1995). This hypothesis is further supported by the observation that mutations in the GTPase domain of dynamin inhibit endocytosis in fibroblasts in a dominant negative manner (Herskovits *et al*., 1993; van der Bliek *et al*., 1993; Damke *et al*., 1994).

How is dynamin recruited to clathrin-coated pits? As well as an N-terminal GTPase domain, dynamin contains a cluster of proline-rich sequences at its C-terminus which have the potential to interact with various Src homology 3 (SH3) domains (Gout *et al*., 1993; Scaife *et al*., 1994; Seedorf *et al*., 1994; Okamoto *et al*., 1997; Figure 1A). SH3 domains are modules commonly found in signal transduction and cytoskeletal proteins. They mediate protein–protein interactions by binding to proline rich sequences that adopt several turns of a type II polyproline helix (reviewed in Pawson and Schlessinger, 1993; Musacchio *et al*., 1994). The proline rich domain of dynamin (PRD) is important both in endocytosis and in its colocalization with clathrin-coated pits, as has been demonstrated by transfection of deletion constructs into fibroblasts (Shpetner *et al*., 1996). Of the many SH3 domain proteins known to interact with dynamin *in vitro*, recent work suggests that the nerve terminal-enriched amphiphysins are major physiological binding partners (for review, see Wigge and McMahon, 1998). Amphiphysin 1 (Amph1) was first identified as a synaptic vesicle-associated protein (Lichte *et al*., 1992) and has since been implicated in the autoimmune disorder, Stiff-Man syndrome (Folli *et al*., 1993; David *et al*., 1994). The interaction of Amph1 with dynamin has a reported affinity of 190 nM, making it one of the strongest SH3 interactions known (Grabs *et al*., 1997). The first direct evidence implicating Amph1 in dynamin recruitment was the dominant negative effect on endocytosis produced by the introduction of amphiphysin SH3 domains into live cells. When transfected into fibroblasts (Wigge *et al*., 1997b) or injected into a lamprey synapse (Shupliakov *et al*., 1997), the Amph1 SH3 domain caused a potent block in clathrin-mediated endocytosis. Coexpression of dynamin I in Amph1 SH3-transfected fibroblasts rescued endocytosis, suggesting that the SH3 domain disrupts the recruitment of dynamin to clathrin-coated pits. Moreover, the SH3 domains of Grb2, spectrin and PLCγ, all of which interact

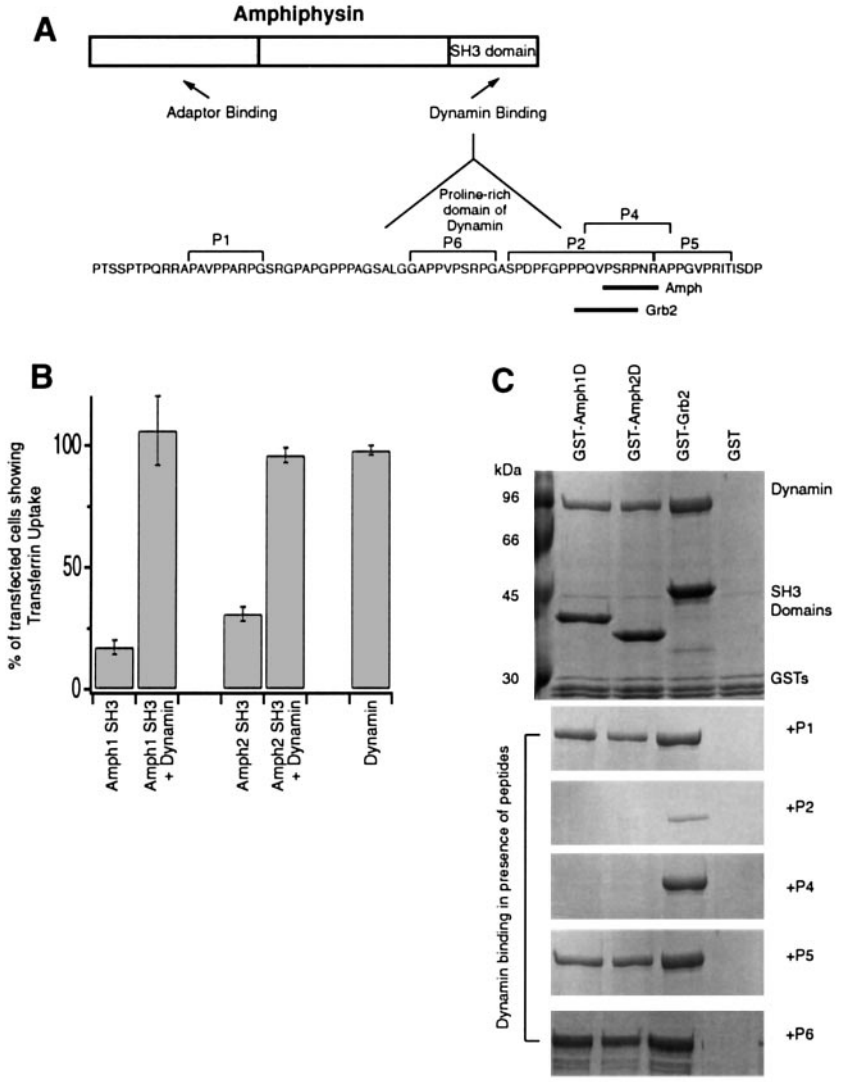

Fig. 1. Specificity and physiological importance of the Amph2–dynamin interaction. (**A**) Schematic representation of the common domain structure of Amph1 and Amph2, along with the sequence of the polyproline region of dynamin with which both isoforms interact. Sequences P1, P2, P4, P5 and P6 indicate the five peptides used for mapping the binding regions, and the solid bars indicate Grb2 N-terminal SH3 and amphiphysin SH3 domain binding sites. (**B**) Overexpression of the Amph2 SH3 domain in fibroblasts inhibits transferrin uptake. COS-7 cells were transiently transfected with the Myc-tagged Amph1 or Amph2 SH3 domain, and/or dynamin, and endocytosed transferrin was visualized as described in Materials and methods. Results are averages of >100 transfected cells ± SEM. (**C**) The SH3 domains of both Amph1 and Amph2 target the same site on dynamin, QVPSRPNRAP. Recombinant SH3 domains, prepared as GST fusion proteins immobilized on glutathione agarose, were incubated with brain extract in the absence of peptide (top panel) or in the presence of 200 μM of each of the peptides P1, P2, P4, P5 and P6. The extent of dynamin binding was assayed by separation of bound proteins by SDS–PAGE, followed by staining with Coomassie Blue.

with dynamin *in vitro*, failed to affect transferrin uptake in this assay (Wigge *et al*., 1997b). Amph1 was previously believed to be a brain-specific protein, but this and other recent work (Volchuk *et al*., 1998) also suggest a more general role for Amph1 in non-neuronal endocytosis.

Recently, we and several other groups have cloned a second amphiphysin isoform, Amph2 (also termed BIN-1 or SH3p9) (Sakamuro *et al*., 1996; Sparks *et al*., 1996; Butler *et al*., 1997; Leprince *et al*., 1997; Ramjaun *et al*., 1997; Tsutsui *et al*., 1997; Wigge *et al*., 1997a). The majority of data indicates that, like Amph1, this isoform participates in clathrin-mediated endocytosis at the plasma membrane. Amph2 contains an SH3 domain, through which it interacts with dynamin (Figure 1A and C), and which displays 51% amino acid identity to that of Amph1 (Leprince *et al*., 1997; Ramjaun *et al*., 1997; Wigge *et al*., 1997a). In brain, the two isoforms are present as a stable heterodimer (Wigge *et al*., 1997a). The role of the amphiphysins in endocytosis is further supported by the finding that they can associate *in vitro* not only with dynamin, but also with several other proteins associated with clathrin-coated pits. These include plasma membrane AP-2 adaptor complexes (David *et al*., 1996; Wigge *et al*., 1997b), clathrin (McMahon *et al*., 1997; Ramjaun *et al*., 1997), synaptojanin (McPherson *et al*., 1996) and SH3p4/endophilin (Micheva *et al*., 1997; Ringstad *et al*., 1997). Furthermore, in nerve terminals KCl-stimulated endocytosis is dependent on the interaction between amphiphysin and dynamin, and is blocked by inhibitors of calcineurin, a phosphatase that dephosphorylates both

Amph1 and Amph2 during stimulation (Marks and McMahon, 1998).

In this paper we show that the SH3 domain of Amph2, like Amph1, inhibits transferrin uptake in fibroblasts and binds to the same sequence on dynamin. We report the 2.2 Å resolution crystal structure of the Amph2 SH3 domain. The structure has several unique features which distinguish it from all the other SH3 domains for which structures have been determined. These include a large patch of negative electrostatic potential (which explains its substrate specificity for multiple arginines in its peptide target sequence) and two extra inserts. Furthermore, we demonstrate that the ability of the amphiphysin SH3 domains to prevent dynamin self assembly in solution is the result of a combination of its unique binding site on dynamin, and an unusually large n-Src loop relative to other SH3 domains. This loop could obstruct dynamin–dynamin interactions important in ring formation. We propose that this unique property of the amphiphysin SH3 domains underlies their ability to block endocytosis *in vivo*, and explains why the SH3 domains of Grb2 and spectrin (which do not prevent ring formation) do not block endocytosis.

Results

The SH3 domain of Amph2 inhibits transferrin endocytosis in fibroblasts

There are two isoforms of amphiphysin, Amph1 and Amph2, which share 49% amino acid sequence identity. We have previously demonstrated the importance of the SH3 domain of Amph1 in dynamin-mediated endocytosis by an uptake assay in fibroblasts which uses transferrin uptake as a marker for endocytosis (Wigge *et al*., 1997b). It is believed that overexpression of this SH3 domain sequesters dynamin, preventing its recruitment and so leaving it unavailable to function in endocytosis. The SH3 domain of Amph2 displays 51% amino acid identity to that of Amph1, and its *in vitro* interaction with dynamin has been well documented (Butler *et al*., 1997; Leprince *et al*., 1997; Ramjaun *et al*., 1997; Wigge *et al*., 1997a). In order to assess its importance and relevance *in vivo*, the SH3 domain of Amph2 was transfected into COS-7 fibroblasts, and its effect on endocytosis was measured by transferrin uptake (see Materials and methods). Figure 1B shows that this SH3 domain-inhibited endocytosis to a similar extent as the Amph1 SH3 domain (transferrin uptake blocked in 69% of cells). Coexpression of dynamin I rescued this effect, suggesting that the Amph2 SH3 domain, like that of Amph1, is acting through sequestration of dynamin into inactive complexes.

The interaction of Amph2 with dynamin is mediated by the sequence PSRPNR on dynamin

At least seven proteins containing SH3 domains bind to dynamin *in vitro* via different polyproline sequences on the C-terminal ~100-residue PRD (Okamoto *et al*., 1997). Amph1 interacts with the sequence PSRPNR at a site partly overlapping the sequence reported to bind to the Grb2 N-terminal SH3 domain (Grabs *et al*., 1997; Okamoto *et al*., 1997; Wigge *et al*., 1997a). In order to identify the binding site for Amph2 and to investigate its relationship to that of Amph1 and Grb2, a number of peptides were designed and synthesized for use in binding studies (Figure 1A). The ability of each of these peptides to inhibit the interaction of rat brain dynamin with the SH3 domains of Amph1, Amph2 or Grb2 was tested *in vitro* (Figure 1C).

Significantly, the only peptides found to abolish amphiphysin binding are P2 and P4, which share the residues QVPSRPNR. Identical results were obtained in peptide competition experiments conducted with affinity-purified dynamin (data not shown). We had previously suggested that the Amph2 binding site on dynamin might show different peptide-binding characteristics from that of Amph1 (Wigge *et al*., 1997a) but the new data demonstrate that the two isoforms do, in fact, bind to the same proline-rich motif on dynamin. Amphiphysin binding to this PSRPNR site is very specific, since peptides P1, P5 and P6 do not compete effectively for the amphiphysin–dynamin interaction (Figure 1C). Clearly, the presence of two arginines on dynamin is crucial for the interaction of the SH3 domains of the amphiphysins. This contrasts with most other dynamin-binding SH3 domains; Grb2 binding is attenuated only by P2, in agreement with other studies showing that the Grb2-binding site on dynamin is three residues N-terminal to the amphiphysin-binding site, and requires only one arginine in the motif PXXPXR (Grabs *et al*., 1997; Okamoto *et al*., 1997). The sequence PSRPXR is present in dynamins II and III as well as dynamin I, suggesting conservation during evolution.

The SH3 domains of Amph1 and Amph2 prevent formation of dynamin rings in solution

The SH3 domains of amphiphysins 1 and 2, although not alone in their ability to bind to dynamin *in vitro*, are the only SH3 domains that can inhibit clathrin-mediated endocytosis when overexpressed in fibroblasts (Wigge *et al*., 1997b). We sought to test whether this special property could be explained by a change in the multimerization state of dynamin upon amphiphysin binding. It has previously been reported that dynamin can be induced to form sedimentable ring-like structures upon dilution or dialysis into low ionic strength buffer (Hinshaw and Schmid, 1995; Carr and Hinshaw, 1997); these are similar to those that form at clathrin-coated pits upon GTPγS treatment (Takei *et al*., 1995). We have used this assay to test the effect of the amphiphysin SH3 domains on the multimerization state of dynamin.

Rat brain dynamin, affinity-purified using immobilized glutathione-*S*-transferase (GST)–Amph2 SH3 as an affinity matrix (see Materials and methods), was first pre-assembled into multimers by dilution into low ionic strength buffer (Buffer C), to a final dynamin concentration of 0.5 μM. To test the effect of the amphiphysins on dynamin multimerization, various recombinant SH3 domains (5 μg each) were then added. After ultracentrifugation at 80 000 *g* to separate assembled multimers from the pool of dynamin remaining in solution, the pellet and supernatant fractions were run on 12.5% SDS–PAGE (Figure 2A). Under control conditions (in the absence of any SH3 domains), a significant fraction (~50%) of the dynamin is pelletable, reflecting an equilibrium between the soluble, dissociated form of dynamin and ring-like multimers. Strikingly, the SH3 domains of both Amph1 and Amph2 disturb this equilibrium, driving most of the dynamin into the non-pelletable fraction. The N-terminal

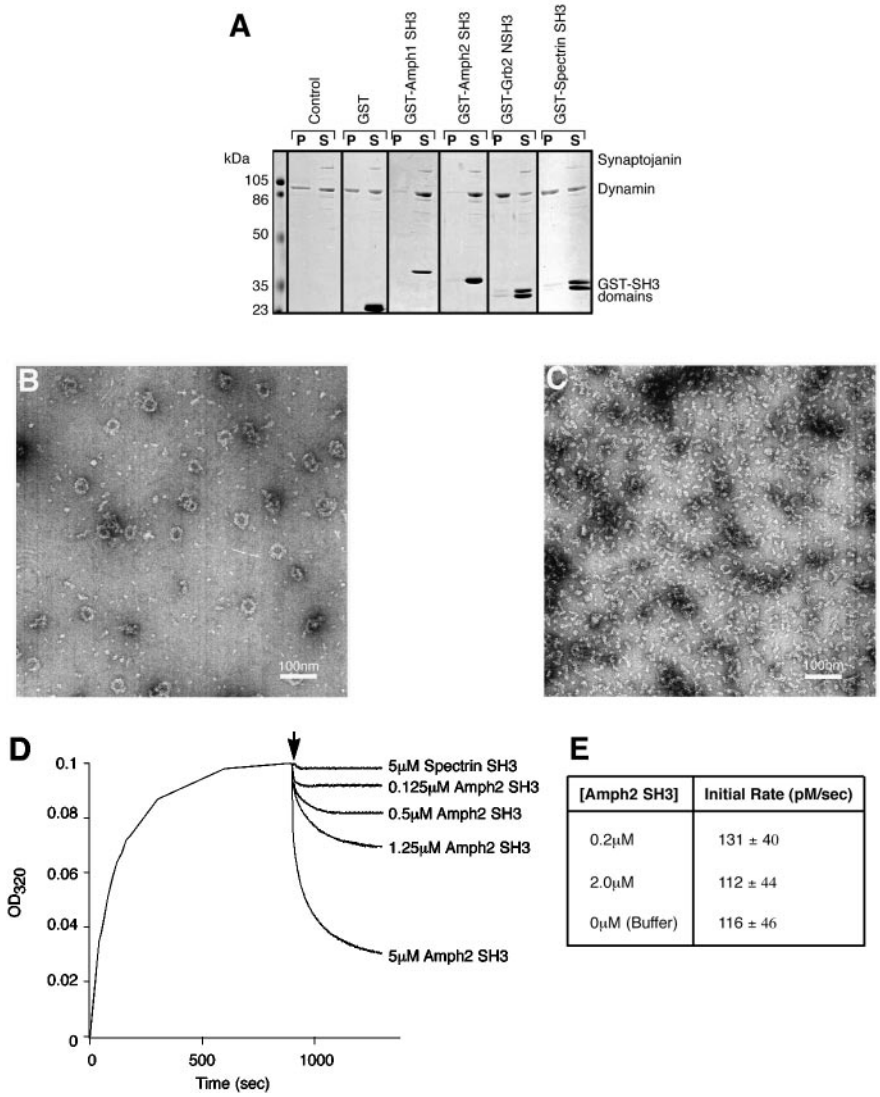

Fig. 2. Prevention of dynamin self-assembly by amphiphysin SH3 domains. (**A**) Amph1 and Amph2 SH3 domains alter the equilibrium of dynamin in favour of the non-multimerized form. Purified dynamin was self-assembled in low ionic strength buffer prior to the addition of various SH3 domains. Multimerized dynamin was pelleted in a sedimentation assay (see Materials and methods); this was analysed together with the soluble dynamin by running pellets (P) and supernatants (S) on SDS–PAGE followed by Coomassie Blue staining. (**B**) Electron micrograph of dynamin pre-assembled in buffer C (see Materials and methods) shows a large proportion of dynamin to be present in ring-like structures. Scale bar represents 100 nm. (**C**) Incubation of preassembled dynamin with the SH3 domain of Amph2 greatly reduces the proportion of dynamin present as rings. Note that this field contains a higher concentration of dynamin than in (B), but most of these molecules are present as small rod-like structures (dissociated dynamin). Scale bar represents 100 nm. (**D**) Kinetics of dynamin 'disassembly' measured by light-scattering. The first part of the graph shows the exponential increase in absorbance characteristic of dynamin self-assembly in low salt buffer. After 20 min, various SH3 domains were added (0.8 μl of various concentrations were added to a total volume of 100 μl) (arrow). The trace shown is representative of three separate experiments. (**E**) The initial rate of dynamin 'disassembly' is independent of [Amph2 SH3]. Initial rates were calculated by curve-fitting traces in (D) to a first-order exponential equation, and by using the conversion 0.1 OD = 0.25 μM multimeric dynamin.

SH3 domain of Grb2 and that of spectrin, both of which bind to dynamin *in vitro* (Gout *et al*., 1993; Wigge *et al*., 1997b) do not result in dynamin ring disassembly. The former actually shifted the equilibrium in the opposite direction, similar to the effects of Grb2 reported previously (Barylko *et al*., 1998). Recombinant hexahistidine-tagged versions of Amph1 and Amph2 disassembled dynamin multimers identically to their corresponding GST fusion proteins, ruling out artefacts due to the GST tag (data not shown).

To ensure that the apparent ring disassembly was not an artefact of this assay, the dynamin structures that formed in low ionic strength were examined by negative-stain electron microscopy (see Materials and methods). Purified dynamin alone formed numerous characteristic rings (Figure 2B) and, less frequently, stacks of rings. In the presence of the Amph2 SH3 domain, there is a smaller proportion of rings (Figure 2C).

Amphiphysin SH3 domains could exert their effect by either (i) binding to the multimeric form and actively disassembling it, or (ii) selectively sequestering the dissociated form, thus displacing the equilibrium and preventing reassembly. In an attempt to distinguish between these two alternatives, the kinetics of disassembly were analysed by a light-scattering assay. Similar assays have been used previously (Warnock *et al*., 1997; Barylko *et al*., 1998), and are sensitive to the sizes of oligomeric complexes as well as their concentration.

Following the addition of dynamin (final concentration 0.5 μM) to low salt buffer (buffer C), OD_{320} increased in an exponential manner to ~0.1 after 20 min, reflecting the self-assembly of dynamin into large multimers, $(D)_n$ (Figure 2D). Upon the addition of recombinant His_6–Amph2 SH3, the light scattering decreased exponentially. Even at sub-stoichiometric levels, the equilibrium of dynamin was affected. The SH3 domain of spectrin did not affect this equilibrium at 5 μM (Figure 2D). The curves were fitted to a single exponential equation $a\ exp(-kt) + c$, from which the apparent initial rates ($-ka$) were extracted. As shown in Figure 2E, the apparent initial rate is independent of amphiphysin concentration. Furthermore, this rate is comparable to the intrinsic dissociation rate of dynamin multimers in the absence of any SH3 domain, seen on dilution of dynamin in an equal volume of buffer ('buffer' in Figure 2E). The fact that addition of increasing amounts of amphiphysin only affected the extent, but did not increase the initial rate, of $(D)_n$ dissociation strongly suggests (but does not prove) that the rate-limiting step is the dissociation of $(D)_n$ rather than the binding of amphiphysin. Thus, rather than actively causing disassembly of $(D)_n$, amphiphysin acts by binding to and sequestering dissociated dynamin molecules, changing the equilibrium and so mediating disassembly indirectly.

Crystal structure of the Amph2 SH3 domain

In this work we have so far demonstrated that the Amph2 SH3 domain, like that of Amph1, is unusual among other SH3 domains in (i) inhibiting endocytosis in fibroblasts, (ii) preventing dynamin multimerization, and (iii) targeting a specific site on the dynamin PRD which contains two arginine residues in the internal packing positions of a polyproline helix (for nomenclature see Lim *et al*., 1994; Wu *et al*., 1995). We now show the molecular basis for these phenomena using the X-ray crystallographic structure of the Amph2 SH3 domain.

The crystal structure of the C-terminal SH3 domain of Amph2 determined by isomorphous replacement (see Materials and methods) is shown in Figure 3A. Its topology is similar to that of other solved SH3 domain structures (for example Musacchio *et al*., 1992; Feng *et al*., 1994; Lim *et al*., 1994; Musacchio *et al*., 1994; Maignan *et al*., 1995; Wu *et al*., 1995), comprising a compact, five-stranded, anti-parallel β-barrel. This core region provides a scaffold on which a number of conserved hydrophobic residues are displayed (shown in pale blue in Figure 3A). As in other structures, the side-chains of these residues, which in Amph2 SH3 are His30, Tyr32, Trp63, Pro86 and Phe89, form prominent hydrophobic surfaces against which the conserved proline residues of the target peptide pack (Figures 3A–C and 4). The interaction of polyproline sequences with SH3 domains generally show a relatively high degree of promiscuity, due to a large contribution from hydrophobic side-chain stacking, itself a low specificity interaction (Wu *et al*., 1995). Specificity in polyproline target sequence recognition is generally provided by interactions between residues in the n-Src and RT loops and those in internal packing positions of the peptide (Figure 3A; nomenclature as Noble *et al*., 1993; Lim *et al*., 1994).

Both Amph2 and Amph1 SH3 domains contain an insertion of 4–5 residues, several of which are acidic, in the n-Src region as compared with other SH3 domains (Figure 3B and C). Another major difference between the structure of Amph2 SH3 and that of other SH3 domains is the presence of a long, ~13-residue insert in the distal loop between β-strands 3 and 4. This insert comprises two short stretches of α helix (residues 68–76 and 78–82) separated by a short section of extended chain. Amph2 SH3 also possesses an N-terminal extension, beyond the commonly accepted SH3 core structure, which interacts with the distal loop insert through hydrophobic side-chain stacking interactions (Figure 3D). This extension, rather than being a loose linker, forms part of the SH3 domain, and indeed there is no protease sensitive region between the SH3 domain and the rest of Amph2 (data not shown). It may thus serve to orient the SH3 domain with respect to the rest of the amphiphysin molecule. The positions of these inserts is illustrated in Figure 3A and B (coloured yellow) and in Figure 3C where the superimposed α-carbon backbone traces of six SH3 domains are shown.

A prominent patch of negative electrostatic potential extends over the peptide binding site

The free energy of binding between proteins includes an electrostatic and a hydrophobic component. Displaying the electrostatic potential and hydrophobicity at the surface of a protein can give information concerning the nature of its interactions with other proteins. In Figure 4, the electrostatic and hydrophobic surface properties of the Amph2 SH3 domain are compared with those of Abl (Musacchio *et al*., 1994) and the Grb2 homologue Sem5 (Lim *et al*., 1994). The most striking aspect of the Amph2 SH3 domain is the large region of negative electrostatic potential (coloured red) at one end of the molecule, replacing a hydrophobic patch in other structures which is involved in interacting with hydrophobic side-chains in their target peptides. This is mainly due to acidic residues in the RT and extended n-Src loops (see Figure 3A and B).

The presence of this larger patch of negative electrostatic potential explains why the Amph2 SH3 domain specifically targets only the site on the PRD of dynamin (PSRPNR) which contains two arginine residues in internal packing positions. The number of exposed acidic residues in the Amph2 SH3 domain would be capable of interacting with more than one arginine side-chain from a polyproline helix. In support of this hypothesis, a similar sequence containing two arginines, PS**R**PI**R,** is found in synaptojanin (p145), the other major *in vitro* binding partner of Amph2. Furthermore, the binding of synaptojanin to Amph2 SH3 is also inhibited by peptide P4 (data not shown). The SH3 domain of Amph1 which targets the same basic sequence in the dynamin PRD has corresponding acidic residues conserved relative to that of Amph2, and therefore is likely to possess a similar acidic patch. The structures of Sem5 N-terminal, Grb2 N-terminal and c-Crk SH3 domains complexed with peptide show that they bind proline-rich sequences which possess a single basic residue at their C-terminal ends (PXXPXBasic) in the 'negative' orientation (Lim *et al*., 1994; reviewed in Wu *et al*., 1995). The basic residue interacts with a small patch of negative electrostatic potential on one side of the molecule (Figure 4) and this ionic interaction provides specificity for the binding (Feng *et al*., 1994; Wu *et al*., 1995). In Amph2 SH3, the larger patch of negative

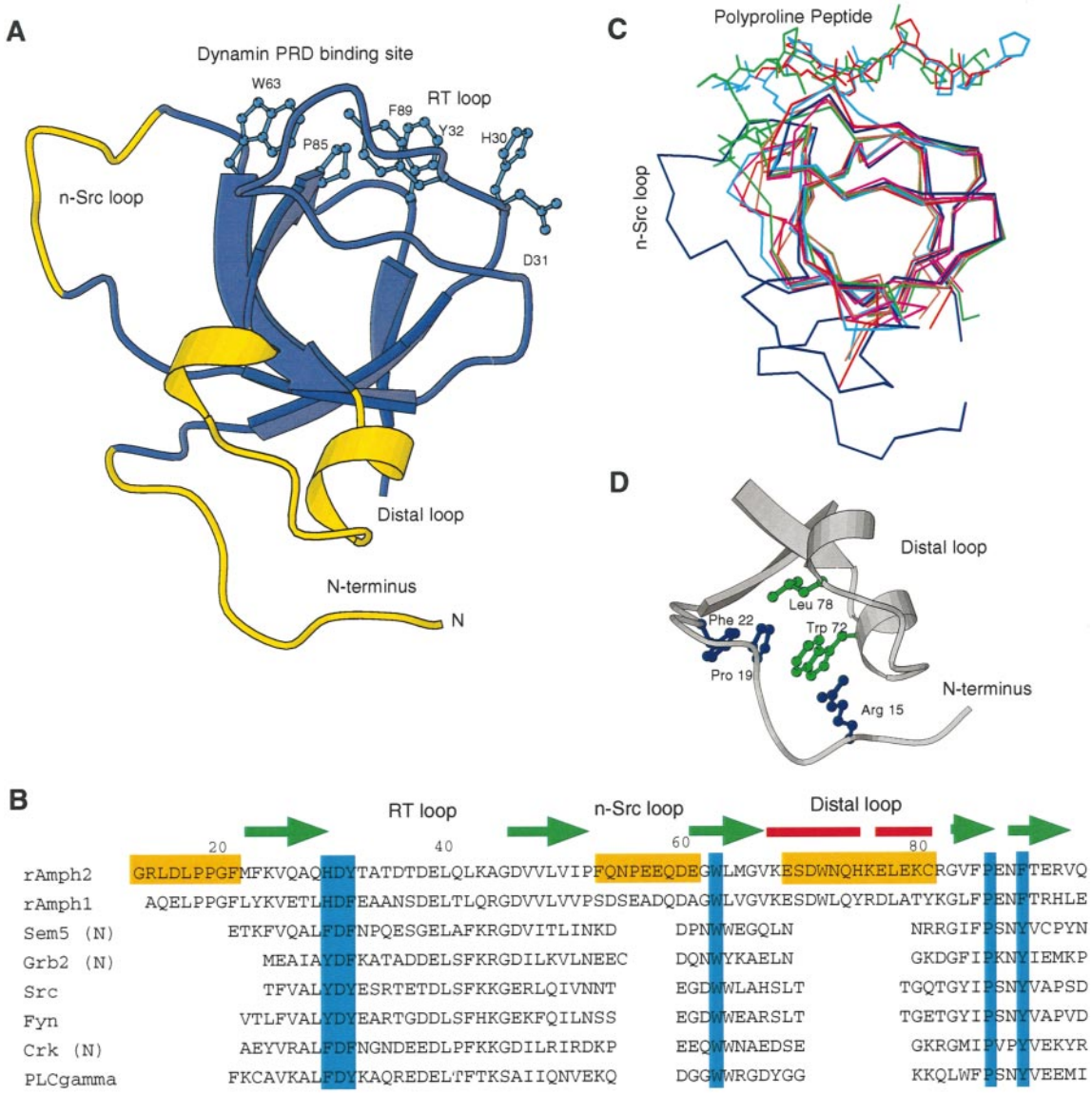

Fig. 3. Structure and sequence alignment of Amph2 SH3 domain. (**A**) Structure of the Amph2 SH3 domain. The peptide backbone of the SH3 domain core [as defined in the sequence alignment in (B)] is shown in dark blue. In both A and B inserts relative to other SH3 domains are shown in gold. Conserved hydrophobic residues involved in binding proline residues are shown in pale blue. The nomenclature of loop regions is derived from Noble *et al*. (1993) and Wu *et al*. (1995). (**B**) Sequence alignment of rat Amph2 SH3 domain, rat Amph1 SH3 domain, N-terminal SH3 domain from *C.elegans* Sem5, N-terminal SH3 domain of rat Grb2, Src SH3 domain, Fyn SH3 domain, Crk N-terminal SH3 domain and PLCgamma SH3 domain. Residue 1 of the Amph2 SH3 domain corresponds to amino acid 494 of the Amph2 deposited sequence (GenBank accession No. Y13380). The secondary structural elements in Amph2 SH3 are shown above its sequence; β strands are shown as green arrows and α helices as red bars. (**C**) Superposition of α carbon traces of SH3 domains from Amph2 (dark blue), Sem5 (red), Fyn (magenta), c-Crk (cyan), spectrin (pink) and Abl (green). The structures of Sem5, c-Crk and Abl are shown with their bound peptides. (**D**) Hydrophobic packing of side-chains in the N-terminus (shown in blue) against those in the distal loop (shown in green).

electrostatic potential is at the same end of the peptide binding site, suggesting that it will bind its target sequence PSRPNR in the same 'negative' orientation.

Residues in the acidic patch are instrumental in dynamin binding in vitro and in vivo

In order to investigate the unusual interaction of Amph2 with dynamin, we made a number of point mutations in the Amph2 SH3 domain (Figure 5A). The mutants fell into two classes: (i) point mutations in hydrophobic residues at positions conserved in all SH3 domains (W63S, F89S, H30S; coloured green), and (ii) mutations of acidic residues thought to be important in coordinating the two arginines on dynamin (namely D36R, D38A, E39K and D60R; coloured magenta). The fold of all the mutants, as determined by circular dichroism measurements, was similar to that of wild-type (data not shown).

The ability of each of these mutants to bind to dynamin was assayed *in vitro* (Figure 5B). Mutations in the conserved hydrophobic residues W63 and F89 abolished dynamin binding, consistent with their conservation in all SH3 domains. Exchanging the histidine at position 30 for a serine reduced binding only by ~75%, suggesting that this histidine is less crucial for dynamin binding than the

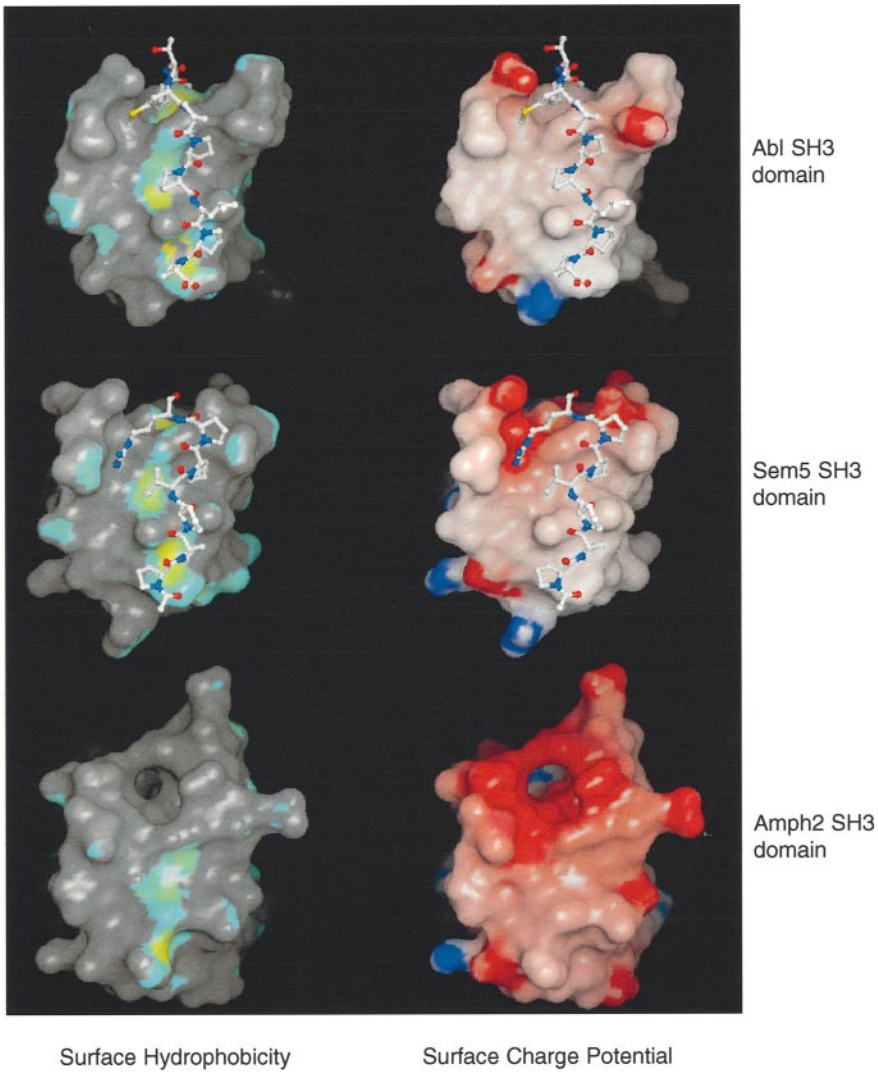

Fig. 4. Surface representations of SH3 domains from Abl, Sem5 and Amph2. The pictures on the left depict surface accessible hydrophobic regions coloured green to yellow for increasing hydrophobicity (M.Noble, X objects, unpublished). Amph2 SH3 shows only two hydrophobic patches as opposed to the three present in Abl and Sem5. On the right are representations of electrostatic potential (created using GRASP) showing the large negatively charged patch (red) on the peptide binding surface (the peptide is shown in the case of Abl and Sem5). The representations show the peptide binding surfaces of the SH3 domains with the n-Src loops pointing toward the top of the page. Coordinates for the SH3 domain of Abl (Musacchio *et al*., 1994) and the N-terminal SH3 domain of sem5 (Lim *et al*., 1994) were obtained from the Protein Data Bank.

other conserved hydrophobic residues. Mutations in the acidic residues Asp38, Glu39 and Asp60 completely abolished dynamin binding, indicating that these are involved in recognition of the PSRPNR sequence. Mutation of Asp36, the only one of the acidic residues in the RT-Src loop not conserved between Amph1 SH3 and Amph2 SH3 does not inhibit dynamin binding.

The interaction of Amph2 SH3 with dynamin is sensitive to pH (Figure 5C). Binding is maximal at pH 7.0, but is greatly reduced when the pH is either raised to 8.5 or lowered to 6.0. An obvious candidate for this effect is His30; however, the H30S mutant exhibits a pH sensitivity similar to wild-type (data not shown). In contrast, the mutant D36R shows reduced pH sensitivity, implying that the pH effect of the interaction is due to ionization of residues in the acidic patch (data not shown). The pK_a of an individual acidic side-chain is normally ~4–5, but may be raised by the proximity of the other negatively charged side-chains in the acidic patch, resulting in a pK_a of 6–8 (a simple example of this effect is shown by the three pK_as of citric acid; 3.13, 4.76 and 6.40).

In order to investigate the effects of these point mutations on the ability of Amph2 SH3 to block endocytosis, COS-7 fibroblasts were transfected with each of the mutants and subsequently assayed for transferrin uptake. All the mutants incapable of binding to dynamin *in vitro* were also unable to inhibit endocytosis (representative examples of both classes of mutation are shown in Figure 6). Interestingly, D36R, the mutant with reduced pH sensitivity to dynamin binding, blocked endocytosis more potently than wild-type. These data confirm that the PRD-binding site of the SH3 domain and its interaction with dynamin are essential for its effect on clathrin-mediated endocytosis *in vivo*. It also suggests that the SH3 domain is not acting by binding another unidentified ligand at a different site.

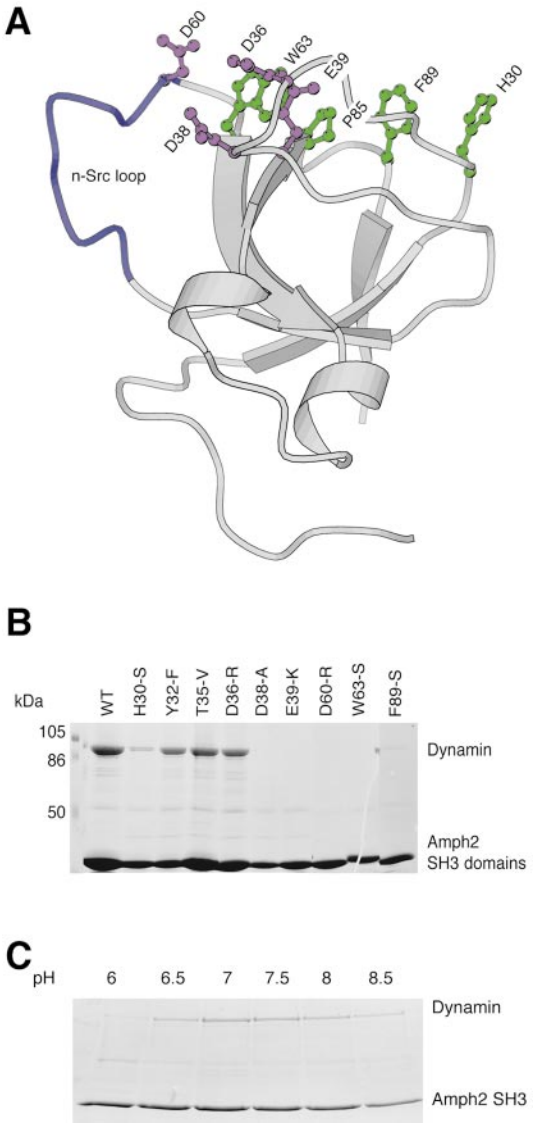

Fig. 5. Point mutations in the Amph2 SH3 domain. (**A**) Structure of Amph2 SH3 showing positions of key mutated residues, coloured according to type. Hydrophobic residues are coloured green and acidic residues in magenta. The longer n-Src loop which is unique to the amphiphysins (the DAPS) that is exchanged for the shorter homologous loop from Grb2 NSH3 is coloured blue. (**B**) Effect of point mutations in GST Amph2 SH3 domain on its ability to bind dynamin. (**C**) Interaction between Amph2 SH3 and dynamin is sensitive to pH. Binding to wild-type is maximal at pH 7.0, but rapidly declines as pH is either increased or decreased.

The extended n-Src loop of the amphiphysins and the prevention of dynamin ring assembly

There are two main features that set the amphiphysin SH3 domains apart from other SH3 domains and may explain why they drive the disassembly of dynamin rings, as shown in Figure 2. First, they are the only SH3 domains so far studied that interact with the sequence PXRPXR at the C-terminus of the dynamin PRD. Secondly, they have two novel inserts, one in the n-Src loop and the other in the distal loop (see Figure 3A and B). While the latter is located on the opposite side of the Amph2 SH3 molecule to the dynamin PRD binding site (and is thus unlikely to effect the binding of dynamin to Amph2 SH3), the extended n-Src loop is adjacent to the dynamin binding site and so is well positioned to interact with a bound dynamin molecule (Figure 3A–C). This loop could play a role in the prevention of dynamin–dynamin interactions essential for ring formation. To address this possibility, we constructed a chimeric Amph2 SH3 domain in which the Amph2 n-Src loop is substituted for that of Grb2 (Amph2–SH3ΔDAPS) such that its n-Src loop is shorter by five residues, i.e. residues 51–60 (PFQNPEEQDE, shown in blue in Figure 5A) being replaced with the equivalent sequence from Grb2 NSH3 (NEECDQ). This mutant binds dynamin with a similar affinity to wild-type (Figure 7A). When tested for its effect in the dynamin multimerization assay, this mutant was markedly less effective than Amph2 at preventing dynamin ring assembly (first two bars in Figure 7B). For convenience, and to distinguish it from other loops in Amph2, we refer to this stretch of residues in the n-Src loop as the dynamin assembly prevention sequence (DAPS). It is likely that the DAPS is acting to sterically inhibit dynamin–dynamin interactions, since it projects beyond the normal boundary of an SH3 domain (Figures 3C and 4). Deleting the extra residues has made the Amph2 SH3 domain more like that of Grb2.

To investigate whether this extended loop plays an important role in endocytosis *in vivo*, the Amph2–SH3ΔDAPS mutant was tested for its ability to inhibit transferrin uptake in fibroblasts. While 78 ± 10% of transfected cells were blocked by the Amph2 SH3 domain, the potency of inhibition caused by transfection of the DAPS mutant was significantly reduced, down to 45 ± 5% of cells blocked (Figure 7C).

As a further test of the importance of the DAPS, we constructed the inverse loop-swap mutant of Grb2 N-terminal SH3 in which its n-Src loop (residues NEECDQ) is replaced with the larger n-Src loop of Amph2 SH3 (residues PFQNPEEQDE; the DAPS). The wild-type SH3 domain weakly promotes the multimerization of dynamin while the chimeric construct (Grb2 NSH3 + DAPS) strikingly favours dynamin ring dissociation (last two bars in Figure 7B). When transfected into fibroblasts, however, the ability of this chimera to inhibit endocytosis was not much greater than that of its wild-type Grb2 NSH3. Preliminary experiments indicate ~82% of cells transfected with Grb2 NSH3 + DAPS exhibit normal transferrin uptake, compared to ~88% for the wild-type construct (data not shown). This result, together with the lack of a complete effect caused by deletion of the DAPS from Amph2, indicates that other factors in addition to this loop may influence the ability of amphiphysin to prevent the multimerization of dynamin. One obvious candidate is the unusual location of the binding site of amphiphysin (PSRPNR) on the PRD of dynamin. Of the cluster of SH3-binding sites on the PRD conserved between dynamin I, II and III, the PSRPNR sequence is in fact the most C-terminal site possible, and may place the SH3 domain in the optimal position to sterically prevent dynamin–dynamin interactions.

Discussion

A dynamin-binding SH3 domain with unique features

In this study we have exploited a combination of structural analysis, mutagenesis, biochemistry and cell biology to

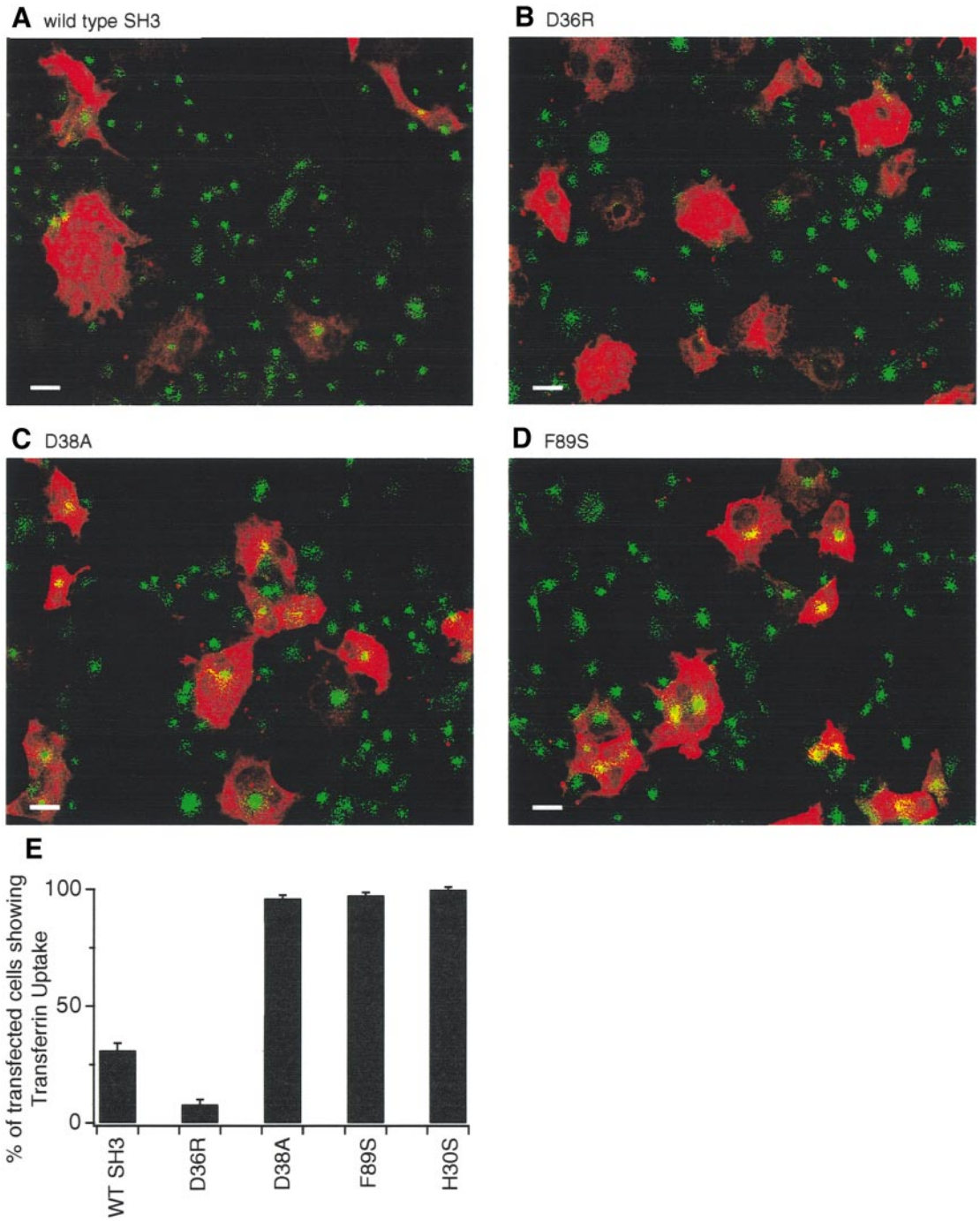

Fig. 6. Effect of mutant forms of Amph2 SH3 domains on transferrin uptake in fibroblasts. Cells transfected with the SH3 domain are stained red and biotinylated transferrin is stained green (see Materials and methods). Amph2 SH3 wild-type and D36R both block transferrin endocytosis but the D36R mutant blocks transferrin uptake in all cells even at low levels of expression (**A** and **B**). Mutants that do not bind dynamin do not block endocytosis [representative examples of mutations in acidic (**C**) and hydrophobic (**D**) residues are shown]. Results are summarized for >100 transfected cells in (**E**). Scale bar represents 10 μm.

seek a better understanding of the protein–protein interactions underlying the action of dynamin and amphiphysin in clathrin-mediated endocytosis.

The crystal structure of the SH3 domain of Amph2 offers an explanation for several interesting results suggesting that the amphiphysin–dynamin interaction is an unusually specific and physiologically important interaction. First, the prominent patch of negative electrostatic potential, which covers much of its peptide binding surface, explains why the Amph2 SH3 domain binds to the PSRPNR sequence of the dynamin PRD—as this is the only site in the PRD in which two arginines would be located on the same face of a polyproline helix. Thus, the ability of both arginine side-chains to contact the surface of the SH3 domain in the context of a polyproline helix defines the specificity of the interaction. Site-directed mutagenesis of several of the acidic residues (Asp38, Glu39, Asp60) demonstrates the importance of this ionic component to the interaction, not only in dynamin binding *in vitro*, but also in the inhibitory effect of the Amph2

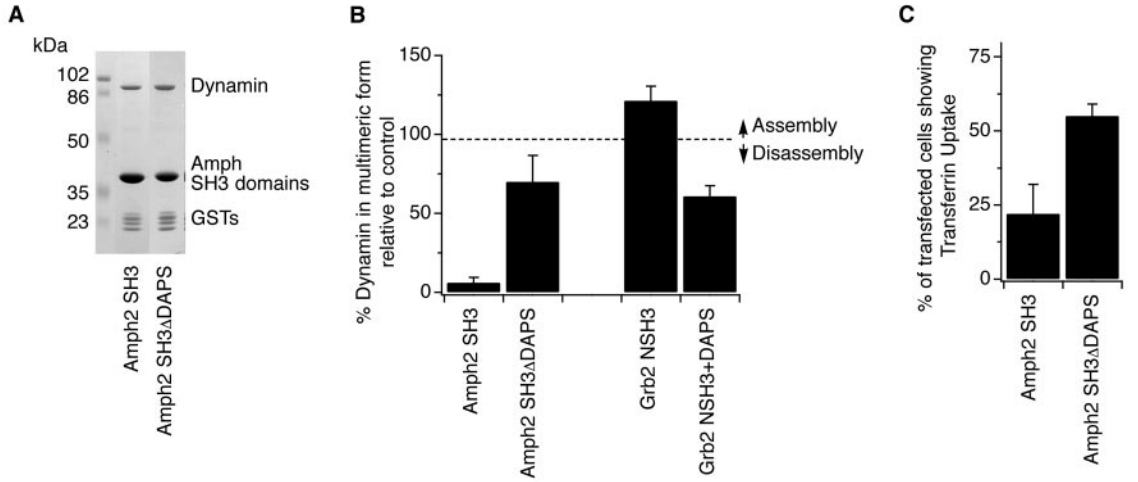

Fig. 7. The DAPS insert in the n-Src loop of Amph2 SH3 underlies its ability to prevent dynamin ring formation. (**A**) Amph2 SH3 and Amph2–SH3ΔDAPS domains bind equally well to dynamin. GST-tagged proteins were incubated with brain extract, containing non-saturating amounts of dynamin, and bound proteins assayed by SDS–PAGE followed by Coomassie staining. (**B**) Amph2 SH3 lacking the DAPS (Amph2–SH3ΔDAPS) is less effective at preventing dynamin multimerization than wild-type Amph2 SH3. Note that the Grb2 N-terminal SH3 domain slightly increases the extent of dynamin multimerization. Insertion of the DAPS into the Grb2 NSH3 domain (Grb2 NSH3 + DAPS) reverses this effect. Results are an average of four experiments ± SEM. (**C**) Importance of the DAPS *in vivo*. The percentage of transfected cells blocked for transferrin uptake is significantly lower for the Amph2ΔDAPS chimera (45 ± 5%) than for the wild-type SH3 domain (78 ± 10%).

SH3 domain on endocytosis *in vivo*. The SH3 domains of both Amph1 and Amph2 are notable for the degree to which pH affects their interaction with dynamin. The optimal pH for binding is 7.0, the same as the intracellular pH measured in neurons (Nachshen and Drapeau, 1988), and declines sharply if the pH is raised or lowered significantly, suggesting that local pH changes at the cell membrane could influence dynamin–amphiphysin interactions.

Control of dynamin ring assembly by the amphiphysins

The amphiphysin SH3 domains, unlike other SH3 domains which are capable of binding dynamin *in vitro* (Gout *et al*., 1993), exert a dominant negative effect on endocytosis in fibroblasts (Wigge *et al*., 1997b). We believe this effect is due to sequestration of endogenous dynamin away from clathrin-coated pits. But why do other SH3 domains that interact with dynamin *in vitro* (Grb2, spectrin and PLCγ) fail to exert any effect on endocytosis *in vivo*? Clearly, there is something quite different about the SH3 domains of the amphiphysins.

Dynamin is thought to exist predominantly in the cytoplasm in a soluble form either as tetramers (Hinshaw and Schmid, 1995; Muhlberg *et al*., 1998) or, possibly, as dimers (Tuma and Collins, 1995) but during endocytosis associates into higher order multimers, thought to be rings, that collar the necks of clathrin-coated pits. It is this multimeric 'ring' form that possesses greatly elevated GTPase activity; the synchronized hydrolysis of GTP in turn is thought to drive a concerted conformational change in the dynamin ring, ultimately resulting in vesicle budding (Hinshaw and Schmid, 1995; Takei *et al*., 1995). Dynamin is therefore continually cycling between its cytoplasmic, dissociated form and the multimeric ring structure at the coated pit, a cycle that of necessity will be both temporally and spatially regulated, and therefore almost certainly require accessory protein factors. Our results suggest that amphiphysin may be one participant in this process, and the presence of a novel insert in the n-Src loop, along with its unique binding site, provide insights into its function.

Unlike the other SH3 domains investigated, those of the amphiphysins alter the equilibrium between the multimeric (ring form) and the dissociated form of dynamin causing disassembly of dynamin rings (Figure 2). We propose that this results from the obstruction of dynamin–dynamin interactions which are crucial for formation of the ring by the extended n-Src loop of the amphiphysin SH3 domain when it is bound in its correct position on the dynamin PRD. Amphiphysin may thus act in a manner akin to the actin monomer-sequestering protein, profilin, which can regulate the polymerization of its binding partner actin *in vitro* (Theriot and Mitchison, 1993). The inhibitory effect of overexpressed Amph1 or Amph2 SH3 domains on endocytosis in fibroblasts now has a more satisfying explanation: these SH3 domains are the only ones to sequester dynamin specifically in a dissociated form. Overexpressed SH3 domains of Grb2 and spectrin can bind to dynamin with a similar affinity, but do not prevent the multimerization of dynamin into rings at the clathrin-coated pit, and so fail to affect endocytosis.

What is the exact role of amphiphysin in endocytosis? A role in the recruitment of dynamin to sites of endocytosis was the first model to be proposed (David *et al*., 1996; Wigge *et al*., 1997b), and is still the most likely one. This hypothesis is supported by two other experiments: (i) microinjection of a peptide that blocks the amphiphysin–dynamin interaction prevents the formation of rings of dynamin at clathrin-coated pits in the lamprey synapse (Shupliakov *et al*., 1997), and (ii) the amphiphysins can interact simultaneously, via different binding sites, with dynamin and AP-2 adaptors (David *et al*., 1996; Wigge *et al*., 1997b), and therefore amphiphysin, positioned at clathrin-coated pits by clustered AP-2 adaptors, could direct dynamin to its correct location at the membrane. Although dynamin has been reported to

bind directly to α-adaptin *in vitro* (Wang *et al*., 1995) (a result that would suggest amphiphysin is not necessary), we have not been able to reproduce this apparently high-affinity interaction (McMahon *et al*., 1997; Wigge *et al*., 1997b). Dynamin may indeed be targeted to clathrin-coated pits via AP-2 adaptors, as shown by the *Drosophila* α-adaptin mutant (Gonzalez-Gaitan and Jackie, 1997), but it is much more likely that the interaction is an indirect one, mediated via amphiphysin as the 'bridging' molecule.

The experiments described in this paper show that amphiphysin selectively binds to dynamin in its dissociated form. While this is not incompatible with a post-budding role in the recycling of dynamin (via disassembly of rings left after the fission reaction), we think it is more probable that amphiphysin acts in the recruitment step, by promoting the efficient targeting of dissociated dynamin to coated pit collars prior to dynamin ring formation. *In vitro* experiments using liposomes (Tuma and Collins, 1995) suggest that a high local concentration of dynamin (probably micromolar) will be required at the neck of the clathrin-coated pit before it can rapidly self-assemble into rings. The observation that amphiphysin can bind to AP-2 adaptors clustered at the coated pit, and the fact that amphiphysin is present in the brain predominantly as a heterodimer (Wigge *et al*., 1997a), makes it likely that its SH3 domains will be concentrated at the coated pit. Indeed, amphiphysin has recently been demonstrated to specifically associate with clathrin-coated pit intermediates, although not as a component of the dynamin ring (Bauerfeind *et al*., 1997). This agrees with our finding that amphiphysin binding and dynamin ring formation are mutually exclusive events. Once multimerized at the neck, dynamin would be predicted to dissociate from the amphiphysin SH3 domains that helped recruit it in the first place. Additional factors important in this process may include the presence of phosphoinositides in the membrane, which bind to the PH domain of dynamin and may shift the equilibrium further towards ring formation (Salim *et al*., 1996; Barylko *et al*., 1998) The scenario we have described would therefore allow a directed, regulated cycle of dynamin recruitment and self-assembly implicit in its function as the molecule controlling vesicle fission.

Conclusion

The crystal structure of the Amph2 SH3 domain has illuminated our understanding of amphiphysin–dynamin interaction and the role it may play in endocytosis. Each isoform in the amphiphysin heterodimer is now known to possess a similar SH3 domain that interacts with dynamin via the same site on the dynamin PRD, PSRPNR. This unusual requirement for two arginines is explained by the large patch of negative electrostatic potential seen in the crystal structure. The n-Src loop projects out from the core of the SH3 domain, and when bound to dynamin obstructs the formation of dynamin–dynamin interactions required for ring formation. We suggest, therefore, that the ability of amphiphysin SH3 domains to recruit dynamin in a controlled fashion, and regulate its self-assembly at the coated pit, will be of significant importance in endocytosis.

Materials and methods

Constructs

The DNA fragment corresponding to the SH3 domain of Amph2 (corresponding to amino acids 494–588 of Amph2 deposited at DDBJ/EMBL/GenBank, accession No. Y13380) was amplified by PCR and cloned into the expression vector pET15b (Novagen), and expressed from the *Escherichia coli* strain BL21 (DE3). Residue 494 of the full length Amph2 was defined as residue 1 of the Amph2 SH3 domain in this paper (to avoid confusion as to which splice form of Amph2 our nomenclature is taken from). The resulting protein contained an N-terminal His_6 tag and a thrombin cleavage site, and had an apparent molecular weight on SDS–PAGE of ~14kDa. This fragment was also cloned into a pCMV-MYC eukaryotic expression vector and into pGex4T for expression as an N-terminal GST fusion protein. The dynamin I construct for expression in COS cells was a kind gift from T.C.Südhof, Dallas, TX (pCMV-96-1a). Rat Grb2 full-length protein, Grb2 N-terminal SH3 domain, and the rat α-spectrin SH3 domain were all cloned by PCR from a rat brain cDNA library using primers as described in Gout *et al*. (1993) into pGex4T and pCMV-MYC.

For large scale bacterial expression His_6Amph2 SH3 single transformants were grown in 2TY medium supplemented with 120 μg/ml ampicillin at 37°C. Expression was induced by the addition of IPTG to a final concentration of 0.3 mM. Cells were harvested after 5 h growth by centrifugation, resuspended in 30 ml buffer per litre of culture [50 mM Tris pH 7.5, 100 mM NaCl, 10 mM β-mercaptoethanol, 0.1 mM phenylmethyl sulfonylfluoride (PMSF), 0.1 mM benzamidine] and lysed by two passes through a French pressure cell. Protein was purified at 4°C by Ni-Agarose affinity, ion exchange (fast-flow Q-sepharose) and gel filtration (Superdex S200) chromatography, giving a final yield of 20 mg purified protein per litre of culture.

Purification of dynamin

Brain extract was prepared by homogenizing rat brains in buffer A [150 mM NaCl, 20 mM HEPES pH 7.4, 4 mM DTT, 0.1 mM PMSF, 0.1 mM benzamidine, 5 μg/ml E64] using 15 ml/brain in a glass-Teflon homogenizer followed by addition of Triton X-100 to a final concentration of 0.1% to complete lysis. Insoluble material was pelleted at 350 000 *g* for 10 min.

A GST fusion protein of the Amph2 SH3 domain was immobilized on glutathione agarose beads and incubated for 1 h with brain extract (1 mg/ml). After washing extensively for 1 h in buffer A, dynamin was eluted with buffer B (1.2 M NaCl, 20 mM PIPES pH 6.2, 10 mM Ca^{2+}, 1 mM DTT) and dialysed overnight into 100 mM NaCl 20 mM HEPES, a method that provided about ~0.2 mg of dynamin per rat brain. Purity was judged to be >95% as assessed by Coomassie Blue staining (see Figure 2A as an example of such a gel).

Protein–protein binding assays

All SH3 domains for use in protein–protein interaction assays were expressed in bacteria as N-terminal fusion proteins with glutathione-*S*-transferase (GST). Protein was purified from bacterial lysates by incubation with glutathione agarose beads in buffer A for 1 h at 4°C followed by extensive washing with buffer A. Twenty micrograms of the purified fusion protein coupled to glutathione beads was then incubated with 0.5 ml of brain extract (prepared as described above) under the desired conditions (presence of peptide, pH) at 4°C. After washing beads three times in buffer A containing 0.1% Triton X-100, bound proteins were analysed by Coomassie Blue staining of 12.5% SDS–polyacrylamide gels.

Dynamin light-scattering assay

Dynamin was diluted to a final concentration of 0.5 μM in buffer C (10 mM NaCl, 20 mM HEPES pH 7.4, 1 mM EDTA, 1 mM DTT) in a 100 μl quartz cuvette (Hellma), and OD_{320} measured after a 10 s lag, at 1 s intervals. After 20 min, at which point an equilibrium was reached between dynamin rings and dissociated dimers or tetramers (~50% of each form), 1 μl of various concentrations of recombinant His–Amph2 SH3 or spectrin-SH3 domain (pre-equilibrated into the same buffer C) were added.

Endocytosis assay and immunocytochemistry

Clathrin mediated endocytosis was measured by assaying transferrin uptake into COS-7 fibroblasts (seen as green perinuclear staining) using biotinylated transferrin and visualized as described previously (Wigge *et al*., 1997b). The Amph2 SH3 domains were MYC-tagged and visualized using the monoclonal antibody 9E10 followed by HRP-anti-mouse, biotinyl-tyramide signal amplification and Texas-red streptavidin (seen as red staining). Transfected cells were compared with untransfected cells in the immediate vicinity. Cells were scored as being blocked only if there was >80% inhibition of transferrin uptake. Therefore the method underestimates the inhibition of transferrin uptake in order to avoid scoring false positives.

Table I. Crystal structure determination

	Native	$Hg(Ac)_2$
Resolution (Å)	2.2	3.0
Unique reflections	5401	1893
Multiplicity	4.2 (3.2)	4.9 (4.1)
Completeness (%)	99.2 (99.7)	98.5 (98.5)
I/σ	4.7 (3.4)	8.2 (4.8)
R_{merge} (%)[a]	9.3 (20.1)	7.2 (14.0)
R_{meas} (%)[b]	10.2 (24.1)	9.0 (17.9)
R_{iso} (%)[c]		32.5
Phasing power		1.29 (0.77)
Anomalous phasing power		1.33 (0.57)
Resolution in outer shell (Å)	2.32–2.20	3.24–3.0
R_{factor}	0.190	
R_{free} (10% of data)	0.258	

Data collection and refinement statistics:
Values in brackets refer to the outer resolution shell.
[a]$R_{merge} = \Sigma\Sigma_i |I_h - I_{hi}| / \Sigma\Sigma_i I_h$ where I_h is the mean intensity for reflection h.
[b]$R_{meas} = \Sigma|(n/n–1)\Sigma_i |I_h - I_{hi}| / \Sigma\Sigma_i I_h$ the multiplicity weighted R_{merge} (Diederichs and Karplus, 1997).
[c]$R_{iso} = \Sigma|F_{PH} - F_P| / \Sigma F_P$, where F_P and F_{PH} are the structure factor for native and derivative, respectively.

Dynamin sedimentation assay

Purified dynamin (50 μg/ml; 0.5 μM) was incubated for 30 min in 200 μl of buffer C in the presence or absence of 100 μg/ml of different recombinant SH3 domains. After ultracentrifugation at 200 000 *g* for 20 min, multimerization was assayed by running pellet (P) or supernatant (S) on 15% SDS–PAGE, followed by Coomassie Blue staining. Under these conditions of low ionic strength, ~50% of the dynamin is in the assembled ring state.

Electron microscopy

Low salt, ring-form dynamin was prepared by dialysis of purified dynamin to 10 mM NaCl, 20 mM HEPES pH 7.5, 1 mM EDTA, 4 mM DTT (buffer C). The protein concentration was adjusted to 0.1 mg/ml with the same buffer, and cross-linking was carried out with 0.5% final concentration of glutaraldehyde for 30 min on ice. To test the effect of Amph2 SH3 on dynamin rings, a 2-fold molar excess of GST–Amph2D in buffer D was incubated with dynamin (final concentration of 0.1 mg/ml), also in buffer C on ice for 30 min. Cross-linking was performed as above. Three microlitres of each sample were applied to air glow-discharged carbon-coated grids, washed in three drops of buffer D, then stained with three drops of 2% uranyl acetate and blotted dry. Micrographs were taken at 40 000× magnification and 80 kV on a Philips EM208 transmission electron microscope, using a defocus of –1 μm.

Crystal structure determination

Crystallization was carried out by hanging drop vapour diffusion at 16°C at a protein concentration of 30 mg/ml by equilibration against a reservoir solution containing 2.0 M ammonium sulfate, 100 mM sodium citrate pH 6.0, 2 mM DTT. Crystals (space group $P3_121$, unit cell 72.14, 72.14, 34.56 Å, γ = 120°) were obtained over a period of 2 weeks with final dimensions 0.3×0.3×0.1 mm in the best cases. X-ray diffraction data were collected at room temperature at SRS Daresbury Station 9.5 (Native) and on a rotating anode [$Hg(OAc)_2$ derivative]. The mercury acetate derivative was obtained by soaking in 2.3 M ammonium sulfate, 100 mM sodium citrate pH 6 containing 1 mM HgOAc for 12 h. All data were recorded on a 300 mM MAR Research image plate and integrated with MOSFLM (Leslie, 1992). Scaling and processing were performed using the CCP4 suite of programs (CCP4). Details are given in Table I.

The single Hg site in the mercury acetate derivative was found by searching the difference Patterson map with Shelxs90 (Sheldrick, 1991). Heavy atom parameters were refined, and phases calculated, with SHARP (de la Fortelle and Bricogne, 1997). Phase improvement and extension from 2.8 to 2.2 Å resolution by solvent flipping and flattening with SOLOMON (Abrahams and Leslie, 1996) led to an excellent electron density map, into which the model was built with O (Jones *et al*., 1991). The model was refined with REFMAC (Murshudov *et al*., 1997) and rebuilt using O. The final model consists of residues 12 –94 (see Figure 3A) plus 51 water molecules. No electron density was found for the first 11 residues of Amph2 SH3, nor for the His_6 tag and thrombin cleavage site. Statistics are given in Table I. Coordinates are available from the Protein Data Bank, accession No. 1BB9.

Extensive attempts to cocrystallize the complex of His_6Amph2 SH3 with peptides P2 and P4 have been unsuccessful. The only conditions in which crystals have been obtained are high ammonium sulfate and low pH, both of which prevent peptide binding in *in vitro* assays, and structures solved from these crystals contain no peptide. Further, the Amph2 SH3 crystals show extensive intermolecular contacts between the peptide binding surfaces across a crystallographic two-fold axis which would be impossible in the presence of peptide.

Acknowledgements

We wish to thank Martin Noble for his determination of surface hydrophobicity, along with Bruno Marks and Michael Stowell for stimulating discussion, and Elizabeth Duke for assistance in collection of data. The MYC 9E10 antibody was a kind gift of S.Munro. D.O. was supported by a Lloyds of London Tercentenary Fellowship.

References

Abrahams,J.P. and Leslie,A.G.W. (1996) Methods used in the structure determination of bovine mitochondrial F1 ATPase. *Acta Crystallogr. D*, 30–42.

Barylko,B., Binns,D., Lin,K.-M., Atkinson,M.A.L., Jameson,D.M., Yin,H.L. and Albanesi,J.P. (1998) Synergistic activation of dynamin GTPase by Grb2 and phosphoinositides. *J. Biol. Chem.*, **273**, 3791–3797.

Bauerfeind,R., Takei,K. and DeCamilli,P. (1997) Amphiphysin I is associated with coated endocytic intermediates and undergoes stimulation-dependent dephosphorylation in nerve terminals. *J. Biol. Chem.*, **272**, 30984–30992.

Butler,M.H., David,C., Ochoa,G.C., Freyberg,Z., Daniell,L., Grabs,D., Cremona,O. and DeCamilli,P. (1997) Amphiphysin II (SH3P9; BIN1), a member of the Amphiphysin/Rvs family, is concentrated in the cortical cytomatrix of axon initial segments and nodes of Ranvier in brain and around T tubules in skeletal muscle. *J. Cell Biol.*, **137**, 1355–1367.

Carr,J.F. and Hinshaw,J.E. (1997) Dynamin assembles into spirals under physiological salt conditions upon the addition of GDP and gamma-phosphate analogues. *J. Biol. Chem.*, **272**, 28030–28035.

Damke,H., Baba,T., Warnock,D.E. and Schmid,S.L. (1994) Induction of mutant dynamin specifically blocks endocytic coated vesicle formation. *J. Cell Biol.*, **127**, 915–934.

David,C., Solimena,M. and DeCamilli,P. (1994) Autoimmunity in Stiff-Man Syndrome with breast cancer is targeted to the C-terminal region of human amphiphysin, a protein similar to the yeast proteins, Rvs167 and Rvs161. *FEBS Lett.*, **351**, 73–79.

David,C., McPherson,P.S., Mundigl,O. and DeCamilli,P. (1996) A role of amphiphysin in synaptic vesicle endocytosis suggested by its binding to dynamin in nerve terminals. *Proc. Natl Acad. Sci. USA*, **93**, 331–335.

de la Fortelle,E. and Bricogne,G. (1997) Maximum-likelihood heavy-atom parameter refinement for multiple isomorphous replacement and multiwavelength anomalous diffraction methods. *Methods Enzymol.*, **276**, 472–494.

DeCamilli,P., Takei,K. and McPherson,P.S. (1995) The function of dynamin in endocytosis. *Curr. Opin. Neurobiol.*, **5**, 559–565.

Diederichs,K. and Karplus,P.A. (1997) Improved R-factors for diffraction data analysis in macromolecular crystallography. *Nature Struct. Biol.*, **4**, 269–275.

Feng,S., Chen,J.K., Yu,H., Simon,J.A. and Schreiber,S.A. (1994) Two binding orientations for peptides to the Src SH3 domain: development of a general model for SH3-ligand interactions. *Science*, **266**, 1241–1247.

Folli,F. *et al.* (1993) Autoantibodies to a 128 kDa synaptic protein in three women with the Stiff-Man syndrome and breast cancer. *New Engl. J. Med.*, **328**, 546–551.

Gonzalez-Gaitan,M. and Jackie,H. (1997) Role of *Drosophila* α-adaptin in presynaptic vesicle recycling. *Cell*, **88**, 767–776.

Gout,I. *et al.* (1993) The GTPase dynamin binds to and is activated by a subset of SH3 domains. *Cell*, **75**, 25–36.

Grabs,D., Slepnev,V.I., Songyang,Z., David,C., Lynch,M., Cantley,L.C. and DeCamilli,P. (1997) The SH3 domain of amphiphysin binds the proline-rich domain of dynamin at a single site that defines a new SH3 binding consensus sequence. *J. Biol. Chem.*, **272**, 13419–13425.

Herskovits,J.S., Burgess,C.C., Obar,R.A. and Vallee,R.B. (1993) Effects of mutant rat dynamin on endocytosis. *J. Cell Biol.*, **122**, 565–578.

Hinshaw,J.E. and Schmid,S.L. (1995) Dynamin self-assembles into rings suggesting a mechanism for coated vesicle budding. *Nature*, **374**, 190–192.

Jones,T.A., Zou,J.Y., Cowan,S.W. and Kjeldgaard,M. (1991) Improved methods for building protein models in electron density maps and the location of errors in these models. *Acta Crystallogr. A*, **47**, 110–119.

Kosaka,T. and Ikeda,K. (1983) Possible temperature-dependent blockage of synaptic vesicle recycling induced by a single gene mutation in *Drosophila*. *J. Neurobiol.*, **14**, 207–225.

Leprince,C., Romero,F., Cussac,D., Vayssiere,B., Berger,R., Tavitian,A. and Camonis,J.H. (1997) A new member of the amphiphysin family connecting endocytosis and signal transduction pathways. *J. Biol. Chem.*, **272**, 15101–15105.

Leslie,A.G.W. (1992) *Recent Changes to the MOSFLM Package for Processing Film and Image Plate Data.* SERC, Daresbury Laboratory, Warrington, UK.

Lichte,B., Veh,R.W., Meyer,H.E. and Kilimann,M.W. (1992) Amphiphysin, a novel protein associated with synaptic vesicles. *EMBO J.*, **11**, 2521–2530.

Lim,W.A., Richards,F.M. and Fox,R.O. (1994) Structural determinants of peptide-binding orientation and of sequence specificity in SH3 domains. *Nature*, **372**, 375–379.

Maignan,S., Guilloteau,J.-P., Fromage,N., Arnoux,B., Becquart,J. and Ducruix,A. (1995) Crystal structure of the mammalian Grb2 adaptor. *Science*, **268**, 291–293.

Marks,B. and McMahon,H.T. (1998) Calcium triggers calcineurin-dependent synaptic vesicle recycling in mammalian nerve terminals. *Curr. Biol.*, **8**, 740–749.

Maycox,P.R., Link,E., Reetz,A., Morris,S.A. and Jahn,R. (1992) Clathrin-coated vesicles in nervous tissue are involved primarily in synaptic vesicle recycling. *J. Cell Biol.*, **118**, 1379–1388.

McClure,S.J. and Robinson,P.J. (1996) Dynamin, endocytosis and intracellular signalling. *Mol. Memb. Biol.*, **13**, 189–215.

McMahon,H.T., Wigge,P. and Smith,C. (1997) Clathrin interacts specifically with amphiphysin and is displaced by dynamin. *FEBS Lett.*, **413**, 319–322.

McPherson,P.S., Garcia,E.P., Slepnev,V.I., David,C., Zhang,X., Grabs,D., Sossin,W.S., Bauerfeind,R., Nemoto,Y. and deCamilli,P. (1996) A presynaptic inositol-5-phosphatase. *Nature*, **379**, 353–357.

Micheva,K.D., Ramjaun,A.R., Kay,B.K. and McPherson,P.S. (1997) SH3 domain-dependent interactions of endophilin with amphiphysin. *FEBS Lett.*, **414**, 308–312.

Morris,S.A. and Schmid,S.L. (1995) The ferrari of endocytosis? *Curr. Biol.*, **5**, 113–115.

Muhlberg,A.B., Warnock,D.E. and Schmid,S.L. (1998) Domain structure and intramolecular regulation of dynamin GTPase. *EMBO J.*, **16**, 6676–6683.

Murshudov,G.N., Vagin,A.A. and Dodson,E.J. (1997) Refinement of macromolecular structures by the maximum-likelihood method. *Acta Crystallogr.* **D53**, 240–255.

Musacchio,A., Noble,M., Pauptit,R., Wierenga,R. and Saraste,M. (1992) Crystal structure of a Src-homology 3 (SH3) domain. *Nature*, **359**, 851–855.

Musacchio,A., Saraste,M. and Wilmanns,M. (1994) High-resolution crystal structures of tyrosine kinase SH3 domains complexed with proline-rich peptides. *Nature Struct. Biol.*, **1**, 546–551.

Nachshen,D.A. and Drapeau,P. (1988) The regulation of cytosolic pH in isolated presynaptic nerve terminals from rat brain. *J. Gen. Physiol.*, **91**, 289–303.

Noble,M.E.M., Musacchio,A., Saraste,M., Courtneidge,A.A. and Wierenga,R.K. (1993) Crystal structure of the SH3 domain in human Fyn; comparison of the three-dimensional structures of SH3 domains in tyrosine kinases and spectrin. *EMBO J.*, **12**, 2617–2624.

Okamoto,P.M., Herskovits,J.S. and Vallee,R.B. (1997) Role of the basic, proline-rich region of dynamin in src homology 3 domain binding and endocytosis. *J. Biol. Chem.*, **272**, 11629–11635.

Pawson,T. and Schlessinger,J. (1993) SH2 and SH3 domains. *Curr. Biol.*, **3**, 434–442.

Pearse,B.M.F. and Robinson,M.S. (1990) Clathrin, adaptors and sorting. *Annu. Rev. Cell Biol.*, **6**, 151–171.

Poodry,C.A. and Edgar,L. (1979) Reversible alterations in the neuromuscular junctions of *Drosophila melanogaster* bearing a temperature-sensitive mutation, shibire. *J. Cell Biol.*, **81**, 520–527.

Ramjaun,A.R., Micheva,K.D., Bouchelet,I. and McPherson,P.S. (1997) Identification and characterisation of a nerve terminal-enriched amphiphysin isoform. *J. Biol. Chem.*, **272**, 16700–16706.

Ringstad,N., Nemoto,Y. and DeCamilli,P. (1997) The SH3p4/SH3p8/SH3p13 protein family: Binding partners for synaptojanin and dynamin via a Grb2-like Src homology 3 domain. *Proc. Natl Acad. Sci. USA*, **94**, 8569–8574.

Sakamuro,D., Elliott,K.J., Wechsler-Reya,R. and Prendergast,G.C. (1996) BIN1 is a novel MYC-interacting protein with features of a tumour suppressor. *Nature Genet.*, **14**, 69–77.

Salim,K., Bottomley,M.J., Querfurth,E., Zvelebil,M.J., Gout,I. and Scaife,R. (1996) Distinct specificity In the recognition of phosphoinositides by the pleckstrin homology domains of dynamin and Brutons tyrosine kinase. *EMBO J.*, **15**, 6241–6250.

Scaife,R., Gout,I., Waterfield,M.D. and Margolis,R.L. (1994) Growth factor-induced binding of dynamin to signal transduction proteins involves sorting to distinct and separate proline-rich dynamin sequences. *EMBO J.*, **13**, 2574–2582.

Seedorf,K., Kostka,G., Lammers,R., Bashkin,P., Daly,R., Burgess,W.H., van-der-Bliek,A.M., Schlessinger,J. and Ullrich,A. (1994) Dynamin binds to SH3 domains of phospholipase Cγ and GRB-2. *J. Biol. Chem.*, **269**, 16009–16014.

Sheldrick,G.M. (1991) In Wolf,W., Evans,P.R. and Leslie,A.G.W. (eds), *Heavy Atom Location Using SHELXS-90*. SERC, Daresbury Laboratory, Warrington, UK, pp. 23–38.

Shpetner,H.S., Herskovits,J.S. and Vallee,R.B. (1996) A binding site for SH3 domains targets dynamin to coated pits. *J. Biol. Chem.*, **271**, 13–16.

Shupliakov,O., Low,P., Grabs,D., Gad,H., Chen,H., David,C., Takei,K., DeCamilli,P. and Brodin,L. (1997) Synaptic vesicle endocytosis impaired by disruption of dynamin–SH3 domain interactions. *Science*, **276**, 259–263.

Sparks,A.B., Hoffman,N.G., McConnell,S.J., Fowlkes,D.M. and Kay,B.K. (1996) Cloning of ligand targets: systematic isolation of SH3 domain-containing proteins. *Nature Biotech.*, **14**, 741–744.

Takei,K., McPherson,P.S., Schmid,S.L. and DeCamilli,P. (1995) Tubular membrane invaginations coated by dynamin rings are induced by GTPγS in nerve terminals. *Nature*, **374**, 186–190.

Theriot,J.A. and Mitchison,T.J. (1993) The three faces of profilin. *Cell*, **75**, 835–838.

Tsutsui,K., Maeda,Y., Tsutsui,K., Seki,S. and Tokunaga,A. (1997) cDNA cloning of a novel amphiphysin isoform and tissue-specific expression of its multiple splice variants. *Biochim. Biophys. Res. Comm.*, **236**, 178–183.

Tuma,P.L. and Collins,C.A. (1995) Dynamin forms polymeric complexes in the presence of lipid vesicles. *J. Biol. Chem.*, **270**, 26707–26714.

van der Bliek,A.M., Redelmeier,T.E., Damke,H., Tisdale,E.J., Meyerowitz, E.M. and Schmid,S.L. (1993) Mutations in human dynamin block an intermediate stage in coated vesicle formation. *J. Cell Biol.*, **122**, 553–563.

Volchuk,A., Narine,S., Foster,L.J., Grabs,D., DeCamilli,P. and Klip,A. (1998) Perturbation of dynamin II with an amphiphysin SH3 domain increases GLUT4 glucose transporters at the plasma membrane in 3T3-L1 adipocytes. *J. Biol. Chem.*, **273**, 8169–8176.

Wang,L.-H., Sudhof,T.C. and Anderson,R.G.W. (1995) The appendage domain of α-adaptin is a high affinity binding site for dynamin. *J. Biol. Chem.*, **270**, 10079–10083.

Warnock,D.E., Baba,T. and Schmid,S.L. (1997) Ubiquitously expressed dynamin-II has a higher intrinsic GTPase activity and a greater propensity for self-assembly than neuronal dynamin-I. *Mol. Biol. Cell*, **8**, 2553–2562.

Wigge,P. and McMahon,H.T. (1998) The amphiphysin family of proteins and their role in endocytosis at the synapse. *Trends Neurosci.*, **21**, 339–344.

Wigge,P., Kohler,K., Vallis,Y., Doyle,C.A., Owen,D., Hunt,S.P. and McMahon,H.T. (1997a) Amphiphysin heterodimers: potential role in clathrin-mediated endocytosis. *Mol. Biol. Cell*, **8**, 2003–2015.

Wigge,P., Vallis,Y. and McMahon,H.T. (1997b) Inhibition of receptor-mediated endocytosis by the amphiphysin SH3 domain. *Curr. Biol.*, **7**, 554–560.

Wu,X., Knudsen,B., Feller,S.M., Zheng,J., Sali,A., Cowburn,D., Hanafusa,H. and Kuriyan,J. (1995) Structural basis for the specific interaction of lysine containing proline-rich peptides with the N-terminal SH3 domain of c-Crk. *Structure*, **3**, 215–226.

Received April 16, 1998; revised June 30, 1998; accepted July 13, 1998